Synthesis, Stability, and Cellular Internalization of Gold Nanoparticles Containing Mixed Peptide–Poly(Ethylene Glycol) Monolayers

ARTICLE *in* ANALYTICAL CHEMISTRY · APRIL 2007

Impact Factor: 5.64 · DOI: 10.1021/ac061578f · Source: PubMed

6 AUTHORS, INCLUDING:

Joseph Anthony Ryan
Iona College
6 PUBLICATIONS **1,359** CITATIONS

SEE PROFILE

Anal. Chem. **2007,** *79,* 2221−2229

Synthesis, Stability, and Cellular Internalization of Gold Nanoparticles Containing Mixed Peptide−Poly(ethylene glycol) Monolayers

Yanli Liu, Mathew K. Shipton, Joseph Ryan, Eric D. Kaufman, Stefan Franzen,* and Daniel L. Feldheim*

Department of Chemistry, North Carolina State University, Raleigh, North Carolina 27695

Gold nanoparticles have shown great promise as therapeutics, therapeutic delivery vectors, and intracellular imaging agents. For many biomedical applications, selective cell and nuclear targeting are desirable, and these remain a significant practical challenge in the use of nanoparticles in vivo. This challenge is being addressed by the incorporation of cell-targeting peptides or antibodies onto the nanoparticle surface, modifications that frequently compromise nanoparticle stability in high ionic strength biological media. We describe herein the assembly of poly(ethylene glycol) (PEG) and mixed peptide/PEG monolayers on gold nanoparticle surfaces. The stability of the resulting bioconjugates in high ionic strength media was characterized as a function of nanoparticle size, PEG length, and monolayer composition. In total, three different thiol-modified PEGs (average molecular weight (MW), 900, 1500, and 5000 g mol^{-1}), four particle diameters (10, 20, 30, and 60 nm), and two cell-targeting peptides were explored. We found that nanoparticle stability increased with increasing PEG length, decreasing nanoparticle diameter, and increasing PEG mole fraction. The order of assembly also played a role in nanoparticle stability. Mixed monolayers prepared via the sequential addition of PEG followed by peptide were more stable than particles prepared via simultaneous coadsorption. Finally, the ability of nanoparticles modified with mixed PEG/RME (RME = receptor-mediated endocytosis) peptide monolayers to target the cytoplasm of HeLa cells was quantified using inductively coupled plasma optical emission spectrometry (ICP-OES). Although it was anticipated that the MW 5000 g mol^{-1} PEG would sterically block peptides from access to the cell membrane compared to the MW 900 PEG, nanoparticles modified with mixed peptide/PEG 5000 monolayers were internalized as efficiently as nanoparticles containing mixed peptide/PEG 900 monolayers. These studies can provide useful cues in the assembly of stable peptide/gold nanoparticle bioconjugates capable of being internalized into cells.

Nanometer-sized metallic, magnetic, and luminescent clusters have emerged as promising materials for probing and manipulating cellular processes. Collectively, they offer nanoscale platforms that can be functionalized with small-molecule drugs, polymers, and biomolecules, and they display a range of important physical properties such as high optical extinctions (gold), stable photoemission (CdSe), superparamagnatism ($CoFe_2O_4$), and the surface-enhanced Raman effect (silver). A few of the exciting applications of nanoclusters documented recently are photothermal ablation of tumors with gold shells,[1] Her2 imaging with quantum dots,[2−4] and magnetic resonance imaging of cells with iron oxide nanoparticles conjugated to the HIV tat peptide.[5]

Applications of nanoclusters in vivo commonly employ antibodies or peptides for selective cell targeting and internalization.[6,7] For example, cell and nuclear targeting by 20 nm diameter gold nanoparticles conjugated to various peptide sequences has been demonstrated.[8,9] In earlier studies, peptides were first covalently bound to the protein bovine serum albumin (BSA), which was subsequently adsorbed onto gold nanoparticles via electrostatic interactions. The use of proteins such as BSA and streptavidin as linkers between peptides or antibodies and nanoparticles is common. However, adsorption thermodynamics and the stability of the resulting gold sol against aggregation in biological media are highly dependent upon the particular peptide sequence chosen. The frequent instability of peptide−BSA−gold nanoparticle conjugates in biological media prompted us to explore PEG-

* To whom correspondence should be addressed. E-mail: Stefan_Franzen@NCSU.edu (S.F.); Daniel.Feldheim@Colorado.edu (D.L.F.).

(1) O'Neal, D. P.; Hirsch, L. R.; Halas, N. J.; Payne, J. D.; West, J. L. *Cancer Lett.* **2004**, *209*, 171−176.
(2) Michalet, X.; Pinaud, F. F.; Bentolila, L. A.; Tsay, J. M.; Doose, S.; Li, J. J.; Sundaresan, G.; Wu, A. M.; Gambhir, S. S.; Weiss, S. *Science* **2005**, *307*, 538−544.
(3) Gao, X. H.; Cui, Y. Y.; Levenson, R. M.; Chung, L. W. K.; Nie, S. M. *Nat. Biotechnol.* **2004**, *22*, 969−976.
(4) Wu, X. Y.; Liu, H. J.; Liu, J. Q.; Haley, K. N.; Treadway, J. A.; Larson, J. P.; Ge, N. F.; Peale, F.; Bruchez, M. P. *Nat. Biotechnol.* **2003**, *21*, 41−46.
(5) Lewin, M.; Carlesso, N.; Tung, C. H.; Tang, X. W.; Cory, D.; Scadden, D. T.; Weissleder, R. *Nat. Biotechnol.* **2000**, *18*, 410−414.
(6) Hirsch, L. R.; Jackson, J. B.; Lee, A.; Halas, N. J.; West, J. *Anal. Chem.* **2003**, *75*, 2377−2381.
(7) Hirsch, L. R.; Stafford, R. J.; Bankson, J. A.; Sershen, S. R.; Rivera, B.; Price, R. E.; Hazle, J. D.; Halas, N. J.; West, J. L. *Proc. Natl. Acad. Sci. U.S.A.* **2003**, *100*, 13549−13554.
(8) Tkachenko, A. G.; Xie, H.; Coleman, D.; Glomm, W.; Ryan, J.; Anderson, M. F.; Franzen, S.; Feldheim, D. L. *J. Am. Chem. Soc.* **2003**, *125*, 4700−4701.
(9) Tkachenko, A. G.; Xie, H.; Liu, Y. L.; Coleman, D.; Ryan, J.; Glomm, W. R.; Shipton, M. K.; Franzen, S.; Feldheim, D. L. *Bioconjugate Chem.* **2004**, *15*, 482−490.

10.1021/ac061578f CCC: $37.00
Published on Web 02/09/2007

Table 1. Peptides Used for Assembling Gold Nanoparticle Conjugates

no.	peptide sequence	origin of peptide	MW	pK_I
I	CGGFSTSLRARKA	adenoviral NLS	1353	12.3
II	CKKKKKKSEDEYPYVPN	adenoviral RME	2084	9.3

based alternative formulation strategies for cell-targeting nanoparticles. One design strategy employs poly(ethylene glycol) (PEG) as a co-adsorbate for peptides attached to gold nanoparticles. The synthesis, characterization, stability, and resistance to protein nonspecific binding of mixed peptide−PEG monolayers on gold nanoparticles are reported here.

EXPERIMENTAL METHODS

All chemicals were used as received from the manufacturer without further purification. Triethylamine and chloroform were purchased from Fisher Chemicals. Gold nanoparticles (10, 20, 30, and 60 nm diameter) were purchased from Ted Pella. Fluorescein isothiocyanate (FITC)-modified IgM and rhodamine (Rh)-labeled BSA were purchased from Fisher. All phosphate-buffered saline (PBS) solutions used were 10 mM unless noted. Eagle's minimum essential medium (EMEM), fetal bovine serum (FBS), and Dulbecco's phosphate-buffered saline (DPBS) were purchased from BioWhittaker. All other solvents and chemicals were purchased from Sigma-Aldrich. All ^{1}H NMR (400 MHz) spectra were recorded at 25.0 °C on a Varian Mercury spectrometer. Infrared spectra (KBr pellet) were taken using a JASCO FT-IR-410 spectrophotometer. UV−visible absorption spectra were acquired on a Hewlett-Packard 8453 Chemstation photodiode array spectrophotometer with attached Chemstation software. Fluorescence intensity data were obtained from a Perkin-Elmer luminescence spectrometer LS50B or BioTek FL-600 plate reader. ζ-potential measurements were performed on a NanoZ Zetasizer with a 633 nm He−Ne laser from Malvern Instrument UK, Inc. Dynamic light scattering (DLS) measurements were obtained on a Malvern Zetasizer 1000. Inductively coupled plasma optical emission spectroscopy (ICP-OES) experiments were performed on a Perkin-Elmer Optima 2100DV optical emission spectrometer.

The peptide sequences investigated in this work (Table 1) were synthesized by The University of North Carolina Peptide Synthesis Facility, purified by HPLC, and supplied in lyophilized form.

Average molecular weight 5000 g/mol thiolated mPEG was purchased from Fluka (PEG 5000). Synthesis of average 900 g/mol and 1500 g/mol ethylene glycols (PEG 900 and PEG 1500, respectively) was accomplished following procedures reported by Tremel[10] (Figure 1).

Synthesis of *p*-Tolylsulfonyl Poly(ethylene glycol) (2). A 0.05 mol amount of poly(ethylene glycol) and an equal molar amount of triethylamine (5.06 g) were dissolved in methylene chloride. To this solution, 9.5 g (0.05 mol) of toluene−*p*-sulfonyl chloride in methylene chloride was added dropwise. The mixture was stirred overnight at room temperature. The white precipitate of triethylamine hydrochloride was filtered off and washed with methylene chloride. The solution was evaporated to dryness and the residue chromatographed on silica gel using a 10:3 ratio of chloroform and acetone. Yield: 48.2% (n = 20), 58.4% (n = 34). ^{1}H NMR: δ 7.76−7.78 (d, 2 H, aromatic), 7.20−7.34 (d, 2 H, aromatic), 4.12−4.15 (t, 2 H, O_2SOCH_2), 3.56−3.68 (m, OCH_2), 2.68 (s, 1 H, -CH_2OH), 2.43 (s, 3 H, -CH_3).

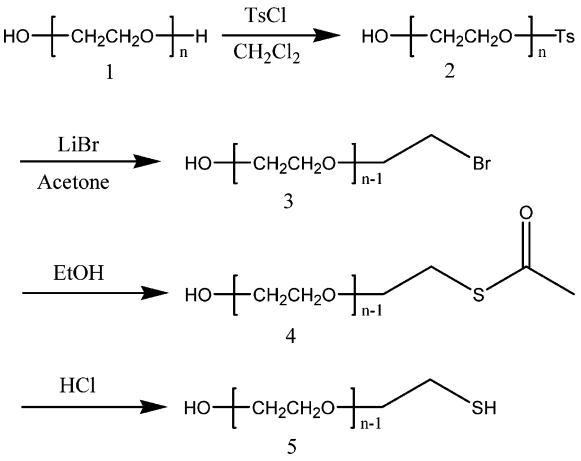

Figure 1. Synthesis of PEG 900 (n = 20) and PEG 1500 (n = 34) molecules.

Synthesis of Bromopoly(ethylene glycol) (3). A 17 g (0.2 mol) amount of LiBr was dissolved in reagent grade acetone. A 21 mmol amount of tosylated alcohol (**2**) was added and the resulting mixture stirred for 5 h at 80 °C. The mixture was then cooled to room temperature and stirred overnight. The solvent was evaporated and chloroform added to the residue. The white precipitate that formed was filtered off, and the solution was washed twice with deionized water. The organic layer was dried over Na_2SO_4, and the solvent was evaporated. Yield: 60.5% (n = 20), 51.0% (n = 34). ^{1}H NMR: δ 3.75 (t, 2 H, CH_2Br), 3.56−3.68 (m, OCH_2), 3.49 (t, 2 H, CH_2OH), 2.68 (s, 1 H, CH_2OH).

Synthesis of Thioacetate (TA)-Protected Poly(ethylene glycol) (4). A 0.01 mol amount of bromonated PEG (**3**) was combined with 1.78 g of potassium thioacetate in a 1:1.2 molar ratio in ethanol. The mixture was stirred under reflux at 80 °C for 5 h. The white KBr precipitate was filtered off and the solvent evaporated. The residue was dissolved in chloroform and washed twice with deionized water. The organic layer was dried over Na_2SO_4, and the solvent was evaporated. Yield: 85.4% (n = 20), 90.2% (n = 34). ^{1}H NMR: δ 2.38 (s, 3 H, CH_3), 3.46−3.78 (m, CH_2O), 2.67 (s, 1 H, CH_2OH).

Synthesis of Mercaptopoly(ethylene glycol) (5). A 1 mmol amount of compound **4** was dissolved in 5 mL of a 1 M solution of hydrochloric acid. The mixture was heated under reflux for 2 h. The solvent was evaporated and the residue dissolved in chloroform. The resulting mixture was washed twice with deionized water and the organic phase dried over Na_2SO_4. Yield: 62.7% (n = 20), 50.4% (n = 34). ^{1}H NMR: δ 3.58−3.74 (m, CH_2O), 3.20−3.23 (t, 2 H, CH_2SH), 2.68 (s, 1 H, CH_2OH), 2.16 (s, 1 H, CH_2SH). IR: 3508 (-OH), 2850−2900 (-CH_2), 1454 (CH_2), 1100−1200 cm^{-1} (C−O−C).

Preparation of PEGylated Gold Nanoparticles. To prepare PEG 5000-modified gold nanoparticles, 145 μL of aqueous PEG 5000 (20 μM) was added to 1 mL of 20 nm citrate-coated gold nanoparticles (1.2 nM), producing a molar ratio of PEG to gold nanoparticles of 2500:1. The mixture was stirred and incubated

(10) Bartz, M.; Kuther, J.; Nelles, G.; Weber, N.; Seshadri, R.; Tremel, W. *J. Mater. Chem.* **1999**, *9*, 1121−1125.

at room temperature for 1 h to allow complete exchange of the citrate with thiol. The mixture was then purified by centrifugation at 13500*g* for 20 min. The supernatant was decanted, and the pellet was resuspended in 1 mL PBS buffer. All other PEGylated nanoparticles were prepared in a similar fashion except that different input ratios of PEG molecules to gold nanoparticles were used to adjust the surface concentration as desired.

Preparation of Gold Nanoparticles with Mixed Monolayers of PEG and Peptides. Two methods were evaluated for preparing mixed monolayers of PEG and peptides on gold nanoparticles: parallel and sequential adsorption methods. In the parallel adsorption method, the desired PEG and peptide were mixed with gold nanoparticles in a molar ratio of 2500:1 (total thiol:particle). For example, 72 μL of 20 μM PEG in PBS buffer and 72 μL of 20 μM cysteine-terminated peptide in PBS were combined and added to 1 mL of 20 nm diameter citrate-capped gold nanoparticles (1.2 nM). The resulting mixture was stirred at room temperature for 1 h to allow complete exchange of citrate with thiol on the particle surface. The complex was washed and centrifuged twice at 11600*g* for 30 min. The supernatant was decanted, and the pellet was resuspended in 1 mL of PBS.

In the sequential adsorption method, PEG thiol was added to a suspension of nanoparticles first, followed by addition of peptide. For example, 250 μL of citrate-capped gold nanoparticles (9.4 nM, 10 nm in diameter) were mixed with 12 μL of PEG 900 (100 μM) at a ratio of PEG to gold nanoparticles of 500:1. The excess PEG molecules were removed by centrifugation at 13000*g* for 15 min. The resulting PEGylated gold nanoparticles were then resuspended in 250 μL of PBS buffer. A 23.5 μL aliquot of peptide (100 μM) was added to produce a molar ratio of peptides to nanoparticles of 1000:1. The mixtures were incubated for 8 h and purified by centrifugation at 13000*g* for 20 min and washed 2× with PBS buffer. The final pellet was resuspended in 250 μL of PBS buffer. UV−visible absorption spectra were then acquired to verify that the nanoparticles did not aggregate during modification and to determine the final concentrations of the nanoparticles.

Determination of Critical Coagulation Concentrations. To determine the critical coagulation concentration (CCC) of PEG- and peptide-modified gold nanoparticles, a series of Eppendorf centrifuge tubes containing 500 μL of identical concentrations of gold nanoparticles (1.2 nM for 20 nm diameter and 9.4 nM for 10 nM) were prepared. Increasing volumes of a 1.7 M NaCl stock solution were added to each sample with the final salt concentration ranging from 20 mM to 1 M. The tubes were vortexed and then allowed to incubate for at least 3 h. Aggregation was assessed by monitoring changes in the characteristic gold nanoparticle plasmon frequency. The threshold NaCl salt concentration in the gold sol, which caused the rapid aggregation of the particles, was determined as the CCC.

Quantifying Peptide Adsorption onto Gold Nanoparticles by Fluorescence Spectroscopy. Gold nanoparticles with mixed monolayers of PEG and peptides were prepared using the parallel or sequential adsorption methods and resuspended in 1 mL of PBS buffer. A 330 μL aliquot of 0.2 mM of aqueous KCN [*Caution!* Handle with care. Do not expose to acidic solution. Ingesting or breathing CN^- can cause death.] was added to oxidatively etch the gold nanoparticles and release the adsorbed monolayer.[11] Complete dissolution of the nanoparticles was indicated by monitoring the disappearance of the gold particle plasmon resonance absorption band at ca. 520 nm. Fluorescence spectra were acquired on the resulting solution, and the average number of peptides per particle was obtained by dividing the measured peptide concentration by the gold nanoparticle concentration.

Characterization of Protein Nonspecific Binding Using Fluorescence Spectroscopy. Gold nanoparticles modified with PEGs or mixed monolayers of PEGs and peptides were prepared following the procedures described above. A 58 μL aliquot of fluorescein isothiocyanate (FITC)-modified IgM (10.0 μM in PBS) or 38 μL of rhodamine (Rh)-labeled BSA (15 μM in PBS) was then mixed with 0.1 mL of modified gold nanoparticles (11.6 nM) to produce a molar ratio of protein to gold particles of 500:1. The mixtures were incubated at room temperature for 30 min and then centrifuged at 13000*g* for 15 min. The supernatant, containing free protein, was gently removed, and the remaining pellet was washed 3× with 500 μL of wash buffer (1% sodium dodecyl sulfate (SDS), 10 mM NaH_2PO_4, 150 mM NaCl, 1 mM ethylenediaminetetraacetic acid (EDTA), pH 7.4). The purified gold nanoparticle pellets were resuspended in 150 μL of PBS buffer, and 50 μL of KCN solution (0.2 mM) was used to dissolve the gold nanoparticles. Fluorescence measurements were performed on (a) a blank (the cyanide-induced dissolution of PEG- or (PEG + peptide)-modified gold nanoparticles), (b) the control (the cyanide-induced dissolution of citrate-modified gold nanoparticles fully coated with protein), and (c) the sample (the cyanide-induced dissolution of PEG- or (PEG + peptide)-modified gold nanoparticles incubated with proteins. Protein standards were prepared by adding known amounts of FITC-IgM or Rh-BSA to solutions of citrate-stabilized gold nanoparticles in PBS, which had been oxidatively converted to soluble $[Au(CN)_4]^{1-}$ by KCN. The calibration curve was used to determine the amount of protein pelleted with, and thus assumed to be nonspecifically adsorbed to, a given sample of pegylated gold nanoparticles. Finally, the average number of protein molecules per particle was obtained by dividing the measured protein molar concentration by the gold nanoparticle concentration.

Cell Treatment with Gold Nanoparticles. The HeLa cell line (obtained from ATCC, Rockville, MD) was maintained in EMEM medium containing 10% fetal bovine serum (FBS) and 1% antibiotics at 37 °C in controlled 5% CO_2 atmosphere. Cells were plated on glass cover slips and grown to ~80% confluency in 12-well plates and then incubated with nanoparticles (10 nm in diameter) for 6 h. Two nanoparticle controls were chosen: gold nanoparticles modified with PEG 900 with input PEG 900:particle mole ratio of 500:1, and particles modified with PEG 5000 with input PEG 5000: particle mole ratio of 250:1. Nanoparticle samples were prepared using the sequential method. PEGylated particles were first prepared using the same PEG:particle ratios as the two control particles. Peptides were then incubated with the particles with input peptide:particle mole ratios of 1000:1 for an additional 8 h. The particles were purified by centrifugation, and the pellet was resuspended in 1 mL of PBS buffer to produce a final concentration of 1.2 nM of gold nanoparticles. The particles were then

(11) Demers, L. M.; Mirkin, C. A.; Mucic, R. C.; Reynolds, R. A.; Letsinger, R. L.; Elghanian, R.; Viswanadham, G. *Anal. Chem.* **2000**, *72*, 5535−5541.

Table 2. Average Molecular Weights and Ethylene Glycol (EG) Units of the PEGs Investigated in This Study

MW (g mol^{-1})	EG Units
900	20
1500	34
5000	114

diluted with EMEM, producing a final particle concentration of ~120 pmol in 1.5 mL of cell media when incubated with cells.

Sample Preparation for Inductively Coupled Plasma Optical Emission Spectroscopy. After 6 h incubation of cells in media containing gold nanoparticles, the cover slips were washed 3× with DPBS, removed from the culture plate, and allowed to dry in air. Dried cover slips were placed in a new well plate, and 500 μL of freshly prepared Optima grade aqua regia was added to each well. [*Caution!* Aqua regia is a strong acid.] The sample remained bathed in aqua regia for 3 h. A 400 μL aliquot of the acid-dissolved samples was placed into individual 15 mL conical tubes containing 3.5 mL of ultrapure water. To quantify the amount of nanoparticle adsorption to the outer cell membrane, control experiments were performed in which cells were treated and washed as described above, but with an additional heparin wash step (5 U/mL). ICP-OES analysis of the samples was then conducted on a Perkin-Elmer Optima 2100DV optical emission spectrometer with a plasma flow of 18 L/min. All standards were made from 100 mg/mL SpexCertiPrep stock solution (Lot No. CL3-19AU).

RESULTS

The objectives of this work were to determine the optimum conditions for assembling stable peptide/PEG gold nanoparticle conjugates and to formulate an empirical understanding of how PEG length and peptide coverage influence cellular internalization efficiency. In total, three different thiol-modified PEGs, four particle diameters (10, 20, 30, and 60 nm), and two peptides (nuclear localization signal (NLS) and receptor-mediated endocytosis (RME)) were explored. The peptides were derived from the adenovirus fiber protein and have been used in previous cell targeting studies.[5,8,9] The peptides were selected because of their demonstrated ability to induce receptor-mediated endocytosis (RME) and nuclear uptake (NLS) in a variety of cell lines when conjugated to gold nanoparticles through bovine serum albumin linkers.[8,9] However, these two peptides have significantly different overall charge, which results in different degrees of destabilization when conjugated to nanoparticles. PEG was chosen because it is a biocompatible material that can improve colloid stability and resistance to protein nonspecific binding.

Assembly of PEG-Coated Gold Nanoparticles. Of initial interest was how PEG length affects the stability of gold nanoparticles in high ionic strength media. Two thiolated PEG molecules were synthesized, which differed in molecular weight (MW) from 900 to 1500 g/mol (Table 2). A commercial PEG with average MW 5000 was also studied.

Gel electrophoresis (1% agarose) was used to qualitatively confirm binding of PEGs to gold nanoparticles. Figure 2 (left) shows a gel image of particles incubated with PEG 5000. The number labeling each lane is the molar ratio of PEG 5000 to gold nanoparticles *input* into the reaction mixture. The gel shift increased with increasing PEG 5000:nanoparticle mole ratios until a plateau was reached between a ratio of 1000 and 2500. Interestingly, the PEG 5000 particles were observed to migrate toward the negative terminal, indicating a net positive charge. Figure 2 (right) shows a gel image of PEG 900-modified nanoparticles. The gel shift decreased with increasing PEG:particle mole ratios, until a plateau was reached at a ratio of 10 000. In contrast to particles modified with PEG 5000, the direction of motion was toward the positive terminal, indicating a net negative charge. A similar saturation and migration behavior was observed with PEG 1500-capped particles.

The ζ-potential of the PEG 5000- and PEG 900-modified nanoparticles was measured in an attempt to better understand the electrophoresis results observed in Figure 2. The ζ-potential measurements showed heterogeneity in that multiple peaks were observed in the data for both PEG conjugates (Supporting Information). The two major peaks for each PEG molecular weight appeared near ca. 0 and −50 mV. Thus, although the two nanoparticle types appear to have opposite charges by gel electrophoresis, very little difference in their overall charge profiles was observed in ζ-potential measurements.

Dynamic light scattering was also used to qualitatively confirm PEG binding. DLS studies of the 20 nm nanoparticles revealed an increase in hydrodynamic diameter as PEG chain length was increased as expected for monolayer formation (Table 3).

Applications of nanoparticles in biology require that they are stable in solutions containing high concentrations of proteins and salts. Gold nanoparticles, however, are highly polarizable metals with a large Hamaker constant. They are prone to aggregation in high ionic strength solutions in which the van der Waals attraction outweighs the electrostatic and/or steric repulsion provided by surface-bound ligands (e.g., citrate or PEG). To determine the stability afforded by PEG ligands, critical coagulation concentrations (CCC) were measured as a function of PEG length, nanoparticle diameter, and the number of PEG molecules added per gold nanoparticle (Figure 3, Table 4, Supporting Information Figure S3). The data show that the CCC of gold nanoparticles depends sensitively upon all of these parameters. Two stability trends are particularly noteworthy from Table 4: (i) for any given PEG length, as the nanoparticle diameter increases, the amount of PEG that must be input into the reaction mixture per nanoparticle increases, and (ii) for any given nanoparticle diameter, as the PEG length decreases, the amount of PEG that must be input into the reaction mixture increases. (This is true despite the fact that any excess PEG was removed prior to performing the CCC tests.) These trends provide useful cues in the construction of stable mixed PEG/peptide gold nanoparticle conjugates (see below).

Nonspecific Binding of Proteins to PEG-Modified Gold Nanoparticles. In addition to improving the stability of gold nanoparticles in high ionic strength media, one potential advantage of PEG monolayers is the prevention of protein adsorption. Indeed, Huang and co-workers reported that PEG 150 (EG_3-SH) prevented the nonspecific binding of proteins such as BSA and lysozyme to

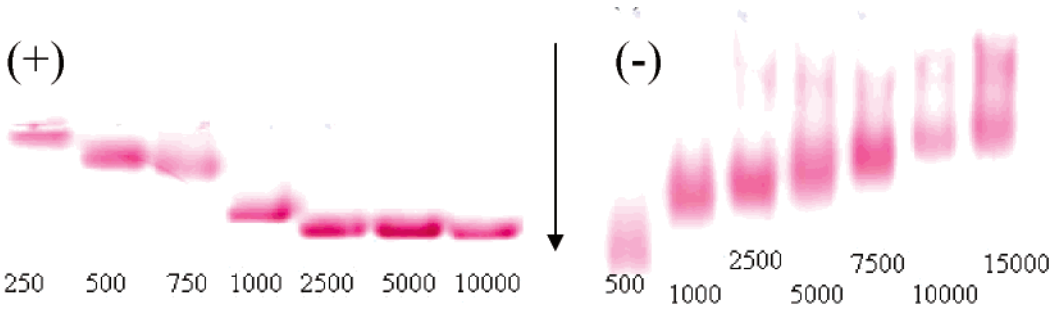

Figure 2. 1% Agarose gel electrophoresis of 20 nm diameter gold nanoparticles following the addition of different ratios of PEG 5000 (left) and PEG 900 (right). The number below each lane indicates the added mole ratio of PEG:gold nanoparticles. The arrow indicates the migration direction.

Table 3. Dynamic Light Scattering (DLS) of 20 nm Diameter Gold Particles Modified with the Indicated Monolayer

monolayer	hydrodynamic diameter (nm)
citrate	21.8 ± 0.5
PEG 900	29.0 ± 0.8
PEG 1500	31.3 ± 1.2
PEG 5000	40.0 ± 0.8

gold nanoparticles.[12−14] Our own gel electrophoresis experiments performed as a control were in accord with those reported previously; that is, gel shifts were not observed between PEG-modified gold nanoparticles incubated in solutions containing BSA or IgM vs protein-free solutions. However, due to the large mass of the gold nanoparticles, gel electrophoresis is not a sensitive method for detecting proteins adsorbed to nanoparticles. Thus a fluorescence assay was developed in order to detect protein nonspecific binding. Indeed, the assay was able to detect BSA or IgM bound to PEG-modified gold nanoparticles, albeit in low amounts (Table 5). To explore a possible correlation between protein nonspecific binding and particle surface area or radius of curvature, four particle diameters were explored. It was found that the number of proteins adsorbed per particle was particle-size-dependent for diameters between 10 and 60 nm, while the adsorbed proteins per unit of surface area was invariant or decreased slightly.

Assembly of Mixed PEG/Peptide Monolayers on Gold Nanoparticles. Having synthesized and characterized pure PEG monolayers on gold nanoparticles, the co-adsorption of PEGs and cell-targeting peptides was investigated. UV−visible absorption spectroscopy and gel electrophoresis confirmed the assembly of particles with mixed monolayers. For example, Figure 4 (left) shows visible spectra of nanoparticles prior to and following modification with a mixed monolayer of PEG 5000 and the RME peptide. The gold nanoparticle plasmon band was shifted by only 4 nm, indicating particle stability following formation of the mixed monolayer. Figure 4 (right) shows the image from agarose gel electrophoresis. The first lane from the left contains particles modified with PEG 5000 alone. The second lane contains particles modified with PEG 5000 and the RME peptide. The gel shift

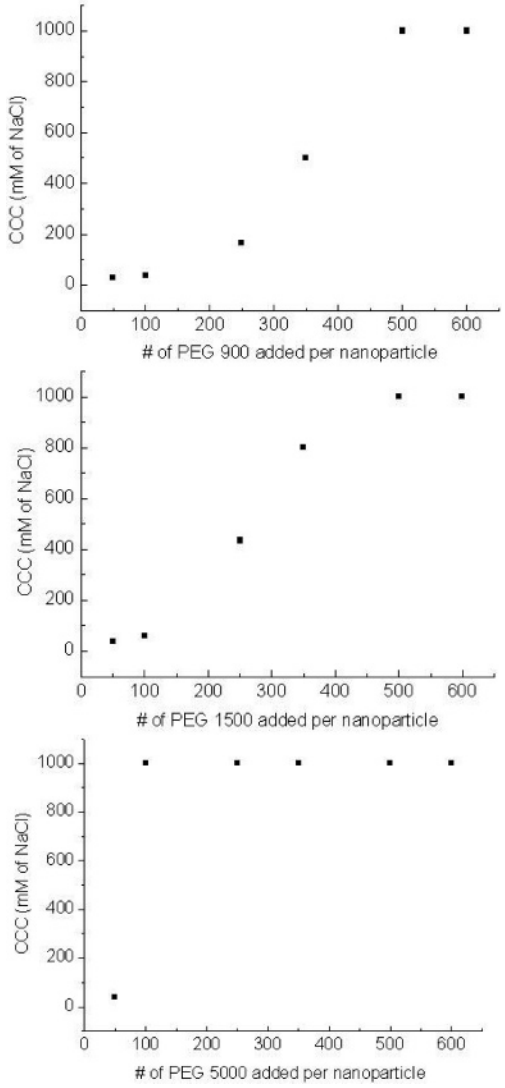

Figure 3. CCC of 10 nm diameter gold nanoparticles modified with PEG molecules.

clearly confirms the formation of a mixed PEG 5000 and RME peptide monolayer.

Fluorescence spectroscopy was employed to quantify peptide loading. Figure 5 is a plot of the number of rhodamine-labeled RME peptides adsorbed per particle after 6 h vs the total number of RME + PEG thiols added to the reaction mixture per particle (added at 1:1 mole ratio). The binding curves are indicative of monolayer adsorption, reaching a plateau at approximately 600

(12) Zheng, M.; Davidson, F.; Huang, X. Y. *J. Am. Chem. Soc.* **2003**, *125*, 7790−7791.
(13) Zheng, M.; Huang, X. Y. *J. Am. Chem. Soc.* **2004**, *126*, 12047−12054.
(14) Zheng, M.; Li, Z. G.; Huang, X. Y. *Langmuir* **2004**, *20*, 4226−4235.

Table 4. Minimum Number of PEG Molecules That Must Be Added into the Reaction Mixture Per Gold Nanoparticle To Form a Stable Gold sol in 1 M NaCl

	no. of PEG molecules required per nanoparticle		
PEG MW	10 nm diameter	20 nm diameter	30 nm diameter
900	500	1000	2500
1500	350	800	2000
5000	100	300	500

Table 5. Nonspecific Binding of Proteins to PEG 5000-Modified Gold Nanoparticles

diameter (nm)	no.of BSA/particle	no. of BSA/μm^2	no. of IgM/particle	no. of IgM/μm^2
10	2 ± 1	6×10^3	3 ± 1	9×10^3
20	7 ± 1	6×10^3	9 ± 2	7×10^3
30	9 ± 3	6×10^3	10 ± 4	6×10^3
60	40 ± 8	3×10^3	50 ± 6	4×10^3

Table 6. CCC of 20 nm Diameter Gold Nanoparticles Modified with Mixed Monolayers of PEG 5000 and the NLS Peptide[a]

PEG:NLS mol ratio	CCC (M)
pure NLS	<0.050
2:8	0.15
3:7	0.20
4:6	>1.0
5:5	>1.0
7:3	>1.0

[a] The conjugates were prepared using the parallel adsorption method and a total thiol to gold nanoparticle mole ratio of 2500:1.

Table 7. CCC of 10 nm Diameter Gold Nanoparticles Modified with Mixed Monolayers of PEG 900 and the RME Peptide[a]

parallel addition method		sequential addition method[b]	
PEG:RME mol ratio	CCC (M NaCl)	PEG:RME mol ratio	CCC (M NaCl)
7:3	0.2	7:3	>1.0
5:5	X	5:5	>1.0
3:7	X	3:7	>1.0

[a] The total thiol:particle mole ratio was 5000:1 for each method. X indicates aggregation immediately upon addition of peptide. [b] PEG added first followed by peptide.

RME peptides per 10 nm diameter nanoparticle when PEG 5000 was the co-adsorbate. Figure S4 shows a similar adsorption isotherm for nanoparticles prepared by the sequential addition method (see Supporting Information).

We have previously observed that the addition of certain peptides to gold nanoparticles can significantly decrease their stabilities in salt solutions.[15] It was thus of interest to determine CCC values for nanoparticles modified with mixed PEG/peptide monolayers. Table 6 shows the stability of nanoparticles modified with mixed monolayers of PEG 5000 and the NLS peptide. The data show that at a constant ratio of total moles of thiol added per mole of gold nanoparticles, increasing the mole ratio of PEG

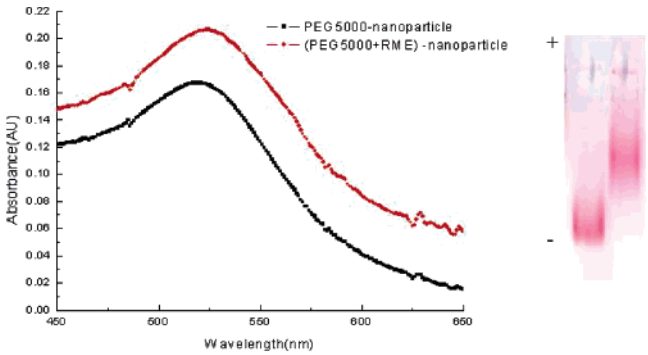

Figure 4. UV−visible absorption spectra of 10 nm diameter gold nanoparticles modified with PEG 5000 and PEG 5000 + RME peptide (left). Agarose gel electrophoresis of gold nanoparticles (right): Left lane contains PEG 5000-modified gold nanoparticles and right lane contains (PEG 5000 + RME peptide)-modified gold nanoparticles. The particles were prepared by sequential method.

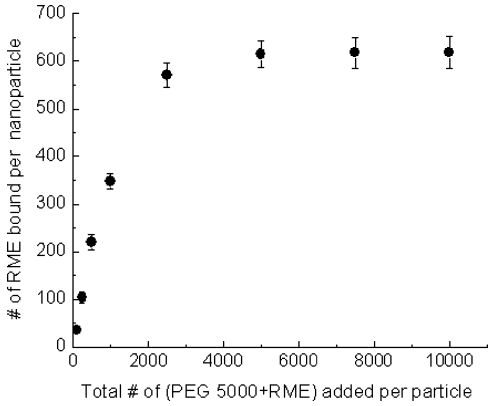

Figure 5. Adsorption isotherm of rhodamine-labeled RME peptide adsorbed onto 10 nm diameter gold nanoparticles. Particles were prepared using the parallel adsorption method. A total thiol to gold nanoparticle mole ratio of 2500:1 was used with an added mole ratio of PEG 5000 to RME of 1:1.

to NLS increased nanoparticle stability. These results motivated us to compare particle stabilities for the two ligand addition methods: parallel vs sequential addition. Mixed PEG/RME monolayers prepared using the parallel thiol addition strategy showed that the larger molecular weight PEG 5000 was able to stabilize gold nanoparticles (10 and 20 nm diameter) in 1 M salt solutions, while the lower molecular weight PEG 900 was not (Table 7). In contrast, mixed monolayers prepared by first adding the PEG followed by the RME peptide were stable for both PEGs studied.

It was shown above that approximately 7% of the surface of a PEGylated 20 nm diameter gold nanoparticle was covered by nonspecifically adsorbed BSA molecules. It was thus of interest to determine whether particles functionalized with PEG *and* peptides could resist protein nonspecific binding as well. This was accomplished by preparing mixed PEG/peptide monolayers of varying mole fraction and incubating them with BSA (Figure S5 of the Supporting Information). The amount of nonspecifically bound BSA was found to be low and relatively independent of the PEG mole fraction and PEG molecular weight (Table 8).

(15) Xie, H.; Tkachenko, A. G.; Glomm, W. R.; Ryan, J. A.; Brennaman, M. K.; Papanikolas, J. M.; Franzen, S.; Feldheim, D. L. *Anal. Chem.* **2003**, *75*, 5797−5805.

Table 8. Nonspecific Binding of Protein BSA to 20 nm Diameter Gold Nanoparticles Modified with the Indicated Monolayer

monolayer	no. of BSA/particle[a]
(PEG 5000 + RME)	11 ± 1
(PEG 900 + RME)	8 ± 1

[a] Average taken over all PEG:RME mole fractions studied (see Figure S5 of the Supporting Information for details).

From the preceding studies, it follows that gold nanoparticle sols containing mixed PEG/peptide monolayers can be assembled and that their stability toward aggregation in high ionic strength media depends upon PEG length. Longer PEGs afford enhanced stability over shorter ones. The function of the targeting peptides was then tested by incubating nanoparticles modified with the RME peptide and either PEG 900 or 5000 with HeLa cells and quantifying cellular internalization using ICP-OES spectroscopy. These studies were designed to determine whether the longer PEG molecules sterically hinder the targeting peptides, thus preventing them from interacting with their target receptors on the cell membrane.

Figure 6 shows the number of 10 nm diameter nanoparticles per well for the mixed monolayer formulations PEG 900 + RME and PEG 5000 + RME prepared using the sequential adsorption method. Both particle formulations were able to enter HeLa cells in 6 h. Surprisingly, particles modified with mixed monolayers of PEG 5000 and the RME peptide were found inside of cells in higher abundance compared to particles modified with PEG 900 and the RME peptide. Control experiments performed on nanoparticles modified with either PEG alone showed comparably less cellular internalization. In an attempt to deconvolute the amount of gold internalized from the amount that may have been nonspecifically adsorbed to the outer cell membrane, control experiments were performed in which the cells were washed with heparin sulfate. The excess heparin was expected to compete effectively with any peptide−gold nanoparticle conjugates adsorbed electrostatically to the outer surface of the cell membrane. Despite this treatment, the total gold observed via ICP-OES was unaffected, suggesting that nanoparticle adsorption to the cell membrane does not contribute significantly to the total gold measured by ICP-OES.

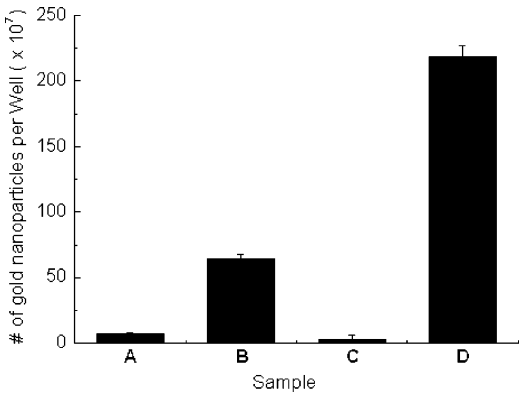

Figure 6. ICP-OES analysis of HeLa cells following 6 h incubation with media containing 10 nm diameter gold particles modified with mixed PEG/RME monolayers. Samples were prepared as follows. (A) PEG 900 to particle mole ratio of 500:1. (B) PEG 900 to particle mole ratio of 500:1 followed by addition of peptide with a mole ratio of 1000:1. (C) PEG 5000 to particle mole ratio of 250:1. (D) PEG 5000 to particle mole ratio of 250:1 followed by the addition of peptide with a mole ratio of 1000:1.

DISCUSSION

Gold nanoparticles have shown great promise as therapeutics, therapeutic delivery vectors, and intracellular imaging agents.[7−9,16−18] For many biomedical applications, selective cell and nuclear targeting is desirable, and this remains a significant practical challenge in the use of nanoparticles in vivo. This challenge is being addressed by the incorporation of cell-targeting peptides or antibodies onto the nanoparticle surface. As these ligands can affect the size, charge, and stability of the resulting bioconjugates, we view studies of monolayer composition−nanoparticle function relationships as being critical to the development of gold nanoparticles that can interface effectively with biological systems.

The systematic studies reported here revealed important differences in the stabilities of gold nanoparticles modified with PEG and mixed PEG/peptide monolayers. We first considered nanoparticles modified solely with PEG monolayers. Gel electrophoresis, DLS, and CCC assays all qualitatively confirmed conjugation of PEGs to gold nanoparticles. Gel electrophoresis revealed opposing migration directions for nanoparticles modified with PEG 900 vs PEG 5000, suggesting that under the conditions in which the gels were run the charge of the two constructs is different, PEG 5000 particles being positively charged. These observations may be due to differences in either the displacement of citrate molecules or the sequestration of cations by the two PEGs. In contrast to the gels, ζ-potential measurements revealed little difference in charge of the two conjugates, although sample heterogeneity made any quantitative conclusions difficult. Thus, while gel shift assays are useful in determining qualitatively the adsorption of PEGs and peptides to gold nanoparticles, the apparent difference in surface potential of these conjugates remains an interesting and important area for further study, particularly insofar as particle charge could influence translocation across cell membranes.

CCC data showed that nanoparticle stability in high ionic strength media depends upon PEG length, nanoparticle diameter, and the ratio of PEG molecules:nanoparticles input into the reaction mixture. Longer PEGs, smaller nanoparticles, and larger PEG:nanoparticle ratios favor more stable sols. The sigmoidal CCC curves reported in Figure 3 suggest that a threshold coverage of PEG must be reached before stability begins to increase. These observations are in accord with DLVO theory, which predicts greater stability for smaller nanoparticles because the van der Waals attraction energy is minimized. Flory−Krigbaum theory also indicates that longer surface-bound ligands and higher ligand coverage will favor sol stability because of increased steric repulsion.[19,20]

The diameter of biomolecule−nanoparticle conjugates is yet another important design parameter, particularly when access to

(16) Rosi, N. L.; Giljohann, D. A.; Thaxton, C. S.; Lytton-Jean, A. K. R.; Han, M. S.; Mirkin, C. A. *Science* **2006**, *312*, 1027−1030.
(17) Hong, R.; Han, G.; Fernandez, J. M.; Kim, B. J.; Forbes, N. S.; Rotello, V. M. *J. Am. Chem. Soc.* **2006**, *128*, 1078−1079.
(18) Kneipp, K.; Kneipp, H.; Kneipp, J. *Acc. Chem. Res.* **2006**, *39*, 443−450.

the cell nucleus is desired. The diameter of the nuclear pore complex in HeLa cell lines is ca. 39 nm.[21] DLS measurements showed that PEGs 900, 1500, and 5000 add 3.5, 5, and 9 nm to the hydrodynamic radius of a gold nanoparticle, respectively. Thus, while PEG 5000 can offer increased stability to 20 nm diameter gold nanoparticles, it could also compromise nuclear translocation efficiency because of its added bulk.

We have also considered nonspecific protein adsorption to PEG-modified gold nanoparticles. The ability of PEG to block proteins from adsorbing onto surfaces has been studied extensively, and it was reported recently that this property translates to PEG-modified gold nanoparticles. In accord with prior results,[12,13] adsorption of PEG-modified gold nanoparticles was not observed using a gel-shift assay. However, a more sensitive fluorescence assay was able to detect the adsorption of BSA and IgM to PEG-modified gold nanoparticles. The measured 7 ± 1 BSAs per 20 nm diameter nanoparticle can be compared to the maximum number of BSA proteins that can be accommodated on a 20 nm diameter citrate-modified gold nanoparticle, approximately 100/nanoparticle.[15] While the absolute number of adsorbed BSA and IgM proteins increased as particle diameter was increased, the number of proteins per unit area remained relatively constant. Thus, within the size regime studied here, there are little inherent differences in particle surface morphology or PEG packing that influence nonspecific protein adsorption.

One of the most compelling attributes of gold nanoparticles is the ease with which mixed thiol monolayers can be assembled on their surfaces.[22] The ability to create mixed monolayers on a nanoscale platform provides a powerful tool that can be used to improve water solubility, tune sterics, and control the trajectory of nanoparticles in cells. Of interest here was whether the addition of PEG as a co-adsorbate could increase the solubility of gold nanoparticles modified with certain cell-targeting peptides (NLS and RME, Table 1).

Mixed peptide/PEG monolayer formation was characterized with gel electrophoresis, fluorescence spectroscopy, and CCC assays. Two methods of monolayer formation were investigated, which differed only in the order in which the thiols were added to gold nanoparticles. Insofar as stability vs aggregation in salt solutions is concerned, nanoparticles prepared using the sequential adsorption method were superior to those prepared by the parallel adsorption route. For example, Table 7 shows that nanoparticles prepared by incubating a gold sol in a solution containing a 1:1 mole ratio of PEG 900 and the RME peptide aggregated rapidly, even without adding excess salt. In contrast, nanoparticles prepared by adding PEG 900 to the gold sol first, followed by addition of the RME peptide, resisted aggregation in solutions containing NaCl at concentrations in excess of 1 M. We suspect that the origin of these marked differences in stability is kinetic. The highly cationic, lysine-rich RME peptide may associate with the anionic gold nanoparticles more rapidly than PEG thiols. As a consequence, the charge on the nanoparticles would be neutralized prior to the formation of a PEG steric barrier. This would be expected to result in nanoparticle aggregation. When even a submonolayer of PEG is attached to the nanoparticle first; however, enough steric repulsion could be created to prevent aggregation upon peptide addition.

Finally, the ability of nanoparticles modified with mixed PEG/RME peptide monolayers to enter HeLa cells was investigated. Given the relative lengths of PEG 5000 and RME peptide, we initially hypothesized that when these two ligands are bound to a nanoparticle, access of the RME signal to its membrane-bound target would be significantly hindered. On the basis of this simple steric argument, we expected less cellular internalization of PEG 5000/RME conjugates vs the corresponding conjugates prepared with PEG 900. ICP-OES analysis of cell uptake showed, however, that the number of PEG 5000/RME conjugates inside HeLa cells after 6 h was nearly a factor of 4 larger than PEG 900/RME conjugates. Even accounting for slight differences in the total number of peptides per nanoparticle (150 RME for PEG 5000/RME conjugates vs 100 for PEG 900/RME conjugates according to their respective isotherms), PEG 5000/RME conjugates enter HeLa cells with surprising efficiency compared to PEG 900/RME conjugates. This could be a manifestation of the larger footprint (lower packing density) of PEG 5000 on a gold surface, relative to PEG 900, a possibility we have attempted to address using a Gaussian chain model for PEG packing on a gold surface.

Assuming the PEG molecules can be modeled as nonentangled Gaussian chains, the average diameter of each PEG is $d = L\sqrt{N}$, where L is the distance between each successive monomer and N is the number of ethylene glycol monomers (-O−CH_2−CH_2-). The distance L is approximately 4.25 Å. For PEGs 900 and 5000 there are 20 and 110 monomer units, respectively. The Gaussian chain lengths for PEGs 900 and 5000 are estimated to be $d = 1.9$ and 4.5 nm, respectively. The surface area of a 20 nm particle is ~1250 nm^2. Assuming that the PEGs bind to the surface such that they sweep out a cone with a tilt angle of approximately 45°, the footprint of each of the PEGs on the surface of the nanoparticle can be estimated to be approximately equal to πr^2, where $r = d/\sqrt{2}$. Therefore, the area covered by the respective PEGs is given by $\pi d^2/2$ so that PEGs 900 and 5000 cover ~6 and ~32 nm^2, respectively. If we assume complete coverage, this implies that the number of PEGs that can bind is ~190 and ~36 for PEG 900 and 5000, respectively (see Supporting Information). For comparison, fully extended chains would be ~8.6 and ~48.2 nm, for PEG 900 and PEG 5000, respectively. DLS measurements in Table 3 show that PEG 900 and PEG 5000 add 3.5 and 9 nm, respectively, to the radius of the particles. These values are in reasonable agreement with the Gaussian chain model but indicate that the chains are constrained on the surface and add more to the radius than the Gaussian chain model would predict. Nonetheless, these considerations give a rough estimate of the substantial differences between the different PEG lengths.

There are several factors that influence the surface charge density and accessibility of targeting peptides on PEG-labeled nanoparticles. On the basis of the smaller size, the packing of PEG 900 is expected to be better than that for PEG 5000. We can think about the packing of PEGs and smaller molecules such as peptides and citrate using a "trees and grass" model. In this model we can envision the exposure of surface groups as depending on the extent to which the larger PEG molecules (trees) can cover

(19) Baudhuin, P. V. d. S. P.; Beauvois, S.; Courtoy, P. J. *Colloidal Gold: Principles, Methods, and Applications*; Academic Press: New York, 1989.
(20) Hunter, R. J. *Foundations of Colloid Science*; Oxford University Press: New York, 1991.
(21) Pante, N.; Kann, M. *Mol. Biol. Cell* **2002**, *13*, 425−434.
(22) Shon, Y. S.; Mazzitelli, C.; Murray, R. W. *Langmuir* **2001**, *17*, 7735−7741.

the smaller molecules near the surface (grass). The poorer packing of the larger PEG molecules likely leads to open areas that can expose peptides for cell targeting.

We can consider the positive charge of the PEG 5000-coated nanoparticle as a second factor that may improve cell-targeting efficiency. PEG 5000/RME conjugates appear to contain a net positive charge, which may provide a favorable interaction with the cell membrane. In contrast, the apparent net negative charge of PEG 900/RME conjugates could hinder its interaction with the cell membrane.

CONCLUSIONS

Mixed PEG/peptide monolayers on gold nanoparticles have been synthesized and characterized for their stability in high ionic strength media. PEG length and particle size are two important adjustable parameters for creating stable peptide/gold nanoparticle conjugates. Although our intuition led to the initial hypothesis that longer PEG co-adsorbates (e.g., MW 5000) would sterically hinder a shorter peptide from accessing cell membrane receptors, this was not born out by experiment. A mixed monolayer consisting of a receptor-mediated endocytic peptide and PEG 5000 was internalized at least as efficiently as the same conjugates with PEG 900 as co-adsorbate.

ACKNOWLEDGMENT

The authors thank the National Institutes of Health (Grant CA098194) for support of this work. We are grateful to Professor Wayne Robarge at NC State for performing ICP-OES measurements.

SUPPORTING INFORMATION AVAILABLE

Additional information as noted in text. This material is avalaible free of charge via the Internet at http://pubs.acs.org.

Received for review August 23, 2006. Accepted December 28, 2006.

AC061578F